Coronal Polarimetry: Determining the Magnetic Origins of Coronal Mass Ejections

Sarah E. Gibson[1], Urszula Bąk-Stęślicka[2], Roberto Casini[1], Joel Dahlin[3], Edward DeLuca[4], Giuliana de Toma[1], Yuhong Fan[1], Judy Karpen[3], Laurel A. Rachmeler[5], Steve Tomczyk[1], Amir Caspi[6], Bin Chen[7], Marcel Corchado-Albelo[8], Samaiyah Farid[1], Nishu Karna[4], Therese Kucera[3], Alin Paraschiv[1], Nour Raouafi[9], Thomas Schad[10] Daniel B. Seaton[5], Shaheda Begum Shaik[11], Maurice Wilson[1], Jie Zhang[11]

[1]NCAR/HAO, [2]Univ. Wroclaw, Poland, [3]NASA/GSFC, [4]SAO,[5]NOAA/NCEI,[6]SwRI, [7]NJIT , [8]CU Boulder, [9]JHU/APL, [10]NSO, [11]GMU

Synopsis: The mechanism for the release of stored magnetic energy in solar eruptions remains a major unsolved problem of Heliophysics. Choosing between triggers requires knowledge of pre-eruptive magnetic fields (**B**). Although linear polarization in visible/infrared (VIR) coronal emission lines reveals intriguing clues about coronal mass ejection (CME) precursor topology, small telescope apertures limit current capability for measuring vector field. **Current coronal observations are insufficient to diagnose 3D coronal magnetic fields in CME precursors.**

Coronal cavities are the ideal candidates for CME precursor studies. B_{LOS} in cavities is a direct measure of stored magnetic free energy, and the presence and location of topological X-points (reconnection locations) and O-points (circulation of **B** about axis) distinguish predictions of the flux rope-torus-instability and sheared-arcade-breakout CME models.

- **Finding:** Coronal cavities are ubiquitous throughout the solar cycle, erupt as CMEs, and have coronal polarimetric signatures that distinguish between model predictions.
- **Recommendation:** Coronal cavities should be targeted in a comprehensive multiwavelength study of CME precursors & associated eruption-driving mechanisms.

Large ground-based VIR telescopes can measure both coronal magnetic field topology and strength through a combination of the saturated Hanle and B_{LOS}-sensitive Zeeman effects.

- **Finding:** The **4m Daniel K. Inouye Solar Telescope (DKIST)** and proposed **1.5m Coronal Solar Magnetism Observatory Large Coronagraph (COSMO-LC)** make a major leap forward in VIR coronal sensitivity, enabling measurement of vector **B.**
- **Recommendation:** A dedicated coronal synoptic telescope with a large field-of-view (i.e., **COSMO-LC**) is needed to identify the dominant CME driving mechanisms, by measuring coronal magnetic fields from precursor state into eruption.

In the UV, a new opportunity has arisen to make use of the strong H I Lyman-α coronal line, which obtains a measurement of **B** that is independent of the Zeeman effect.

- **Finding:** Small-telescope spectropolarimetric capability in the unsaturated Hanle regime provides an independent and complementary coronal magnetic diagnostic to large ground-based telescope measurements.
- **Recommendation:** The proposed 12-cm **Coronal Lyman-α Resonance Observatory (CLARO)** spectropolarimetric coronagraph demonstrates a path forward for space-based observations of the coronal magnetic field that should be incorporated into future missions away from the Sun-Earth line (e.g., **COMPLETE**).

1. The Problem: Why Do CMEs Erupt?

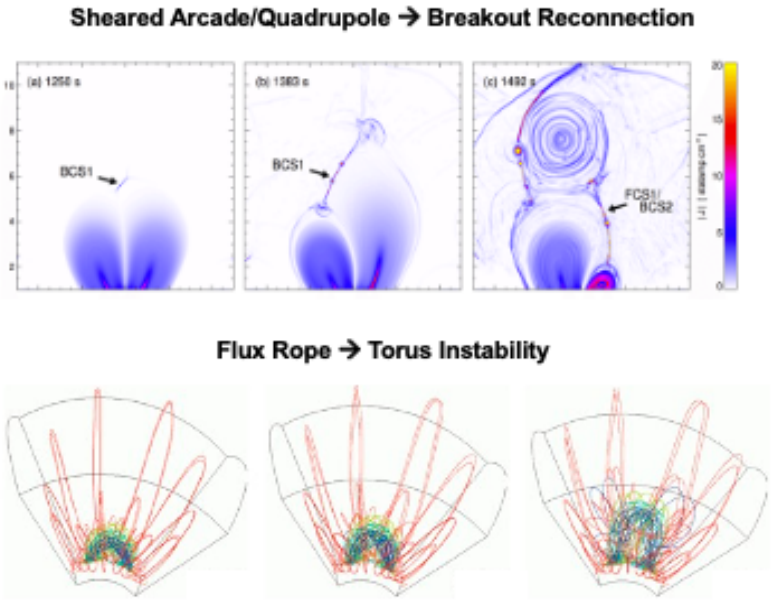

Fig. 1. The mechanism for the release of stored magnetic energy in solar eruptions remains a major unsolved problem of Heliophysics. (Top) Current density magnitude vs time, illustrating the reconnection-driven breakout eruption scenario (Lynch et al. 2016; high-res). (Bottom) Ideal torus instability triggering eruption in a magnetic flux rope (Fan & Gibson 2007; high-res.)

Coronal mass ejections (CMEs) are solar eruptions associated with potentially devastating space weather. CMEs are thought to be driven by the free energy stored in twisted or sheared magnetic fields, but the mechanism underlying the release of this energy remains controversial. The key issue of solving the controversy and determining the CME mechanism has boiled down to identifying the coronal magnetic configuration prior to the eruption (Patsourakos et al. 2020). One scenario depends on magnetic reconnection above a multipolar magnetic structure (breakout reconnection, e.g., Antiochos et al. 1999; Fig. 1, top). Here, a sheared magnetic field pushes up against a critical topological point (oppositely directed magnetic fields, i.e., an **X-point**), forming a current sheet. Reconnection at this sheet removes the overlying field, enabling the energized, sheared field to erupt outward after forming a flux rope. Another type of model involves a pre-existing magnetic flux rope (where magnetic field circulates about an axis, i.e., an **O-point**) which undergoes the ideal torus instability as the flux rope axis rises past a critical point in the gradient of the overlying magnetic field (Kliem & Török 2006; Fan & Gibson 2007; Fig. 1, bottom). **Choosing between models is essential for space weather prediction but requires knowledge of CME precursor topology, i.e., the existence and location of X- and O-points[1].**

Determining the coronal magnetic field from solar surface measurements is difficult for several reasons. If simplifying assumptions such as the current-free or potential limit to the magnetic field in the corona are made, a unique solution can be determined that yields a good first-order characterization of the global coronal magnetic field but ignores the energy-carrying currents that

[1] Note that small O- and X-points may exist within current sheets during eruption (Karpen et al. 2012, Lynch et al., 2016). In this white paper we are using the terms to refer to larger topological features associated with CME precursors, namely the circulation of magnetic fields around a line-of-sight-aligned axis (O-point) and the null point at the top of a multipolar (pseudostreamer) structure where breakout reconnection is likely to occur (X-point).

drive the CME. Vector magnetic information at the photospheric boundary can be used to solve for a non-linear force-free field (NLFFF), but since the photospheric field is not force-free (i.e., not magnetically dominated), these models are prone to inconsistencies and non-uniqueness (de Rosa et al. 2009). **The photospheric boundary alone is insufficient to constrain the coronal magnetic field, motivating polarimetric observations in the corona.**

A range of multiwavelength (radio, visible/infrared (VIR), ultraviolet (UV)) measurements yield direct information on the coronal magnetic field through sensitivities to a variety of physical mechanisms (Gibson et al. 2021; see Table 1). However, the only daily synoptic coronal magnetic diagnostics obtained to date have been measurements of linear polarization by the Coronal Multichannel Polarimeter (CoMP) (Tomczyk et al. 2008) and its replacement, the Upgraded CoMP (UCOMP). Since the VIR lines accessible to the ground are from *forbidden* transitions that lie in the saturated regime of the Hanle effect (Casini & Judge 1999), these measurements determine magnetic field plane-of-sky (POS) direction but not the magnetic strength. Even so, measurements of linear polarization consistently demonstrate a "lagomorphic" (rabbit-head-shaped) structure as predicted for forward-modeled magnetic flux ropes (Fig. 2; Bąk-Stęślicka et al. 2013). This indicates the presence of line-of-sight magnetic field (B_{LOS}) in cavities, but is not sufficient to confirm the presence of a magnetic O-point (Rachmeler et al. 2012). **Linear polarization of coronal VIR lines reveals structures consistent with magnetic flux ropes, but identifying magnetic O-point location ultimately requires measuring B_{LOS}.**

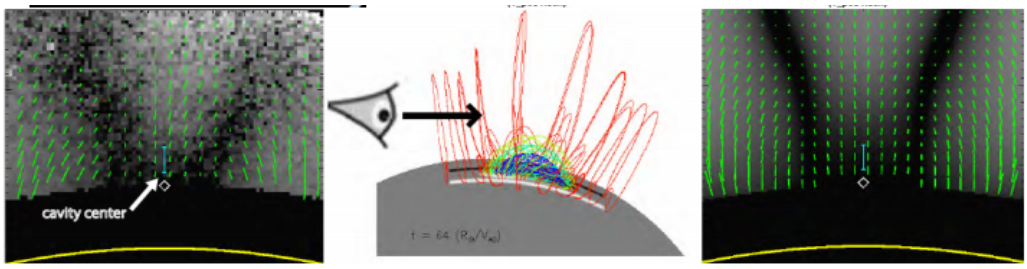

Fig. 2. CoMP observes a lagomorphic morphology in linear polarization. CoMP Fe XIII observations (left) are consistent with synthetic data (right) from a magnetic flux rope model (middle; Bąk-Stęślicka et al. 2013; high-res). The dark "rabbit ears" appear where the POS magnetic field crosses the van Vleck angle of 54.74° and linear polarization rotates 90° (green linear polarization vectors). The dark "rabbit head" occurs because of a combination of van Vleck angle crossing and line-of-sight aligned magnetic field at the flux rope axis, complicating precise identification of the O-point location.

Multipolar magnetic structures have their own distinctive signatures in FeXIII linear polarization, as the van Vleck effect creates lobes converging at the X-point (Rachmeler et al. 2013; Fig. 3b-c). A sheared arcade-quadrupolar simulation leading to magnetic breakout (Dahlin et al. 2021) predicts a structure of this nature, in which the magnetic X-point is shifted asymmetrically in response to different degrees of shear in the magnetic lobes (Fig. 3d). Such structures are observed by CoMP in association with coronal pseudostreamers (e.g., Gibson et al. 2017; Fig. 3a,e), although the precise location of the X-point can be difficult to ascertain (Fig. 3e). **Linear polarization in VIR coronal emission lines can reveal X-points, but current observations are limited by telescope aperture in resolving these features.**

Recently and for the first time, the POS component of coronal magnetic fields was mapped using VIR coronal seismology (Yang et al. 2020a, 2020b). Analytical (Plowman 2014, Dima & Schad 2020) and forward-model (Dalmasse et al. 2019; Paraschiv & Judge 2022) capabilities for inverting full vector magnetic fields are currently maturing but depend on measuring the circular polarization, sensitive to B_{LOS}. However, circularly polarized light is extremely faint in the VIR corona, making its detection with small-to-medium aperture telescopes extremely rare (Lin et al. 2000, 2004). In radio, the Expanded Owens Valley Solar Array (EOVSA) is enabling unprecedented measurements of coronal magnetism during solar flares (Chen et al. 2020; see *white paper by Chen et al. 2022* for discussion of future directions in radio). At UV wavelengths, measurements may be made in the unsaturated Hanle regime of *permitted* transitions and utilized to diagnose magnetic field direction and strength (Bommier & Sahal-Brechot 1982; Fineschi et al. 1991; 1993; Casini et al. 2017; Trujillo Bueno et al. 2017), but to date these have only been obtained in the upper chromosphere and transition region (Woodgate et al. 1980; West et al. 2006; Ishikawa et al. 2021; Kano et al. 2017). The only UV coronal spectropolarimetric observation was a very special case in which the solar and heliospheric observatory (SOHO) satellite rotated, serendipitously turning the Solar Ultraviolet Measurements of Emitted Radiation (SUMER) instrument into an effective (if somewhat inefficient) spectropolarimeter (Raouafi et al. 2002). **Coronal observations to date have not been sufficient to diagnose the 3D coronal magnetic field in CME precursors.**

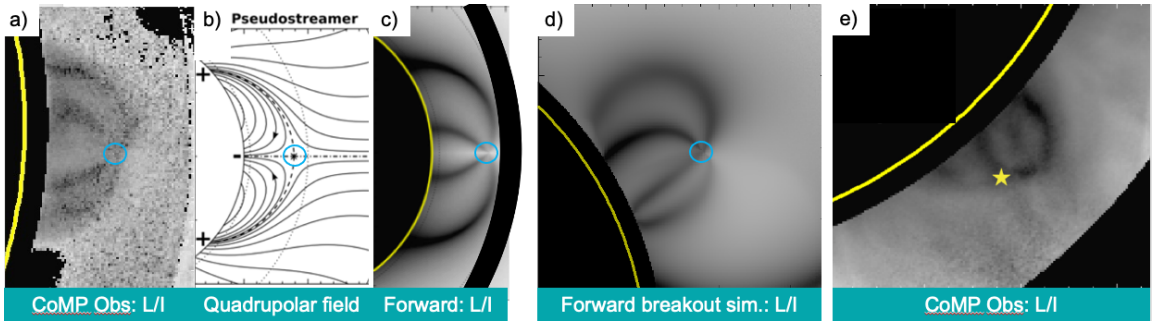

Fig. 3. Pseudostreamers (quadrupolar structures) and associated magnetic X-points can be diagnosed with linear polarization of VIR coronal emission lines. a) CoMP FeXIII linear polarization fraction (L/I) for a pseudostreamer (Gibson et al. 2017). b) Quadrupolar magnetic field lines and c) predicted L/I signature (Rachmeler et al. 2013). d) Forward-modeled L/I for sheared arcade/breakout simulation (Dahlin et al. 2021; see also Fig. 5 (bottom)). Blue circles indicate X-point location. e) A less symmetric CoMP pseudostreamer with X-point tentatively identified (star). High-res a-c; e.

2. The Solution, Part One: Coronal Cavities as CME precursors

Coronal prominences (a.k.a. filaments when observed on the solar disk) often erupt in CMEs, but these mass-loaded structures trace only a small portion of the 3D fields that encompass them. Filament channels are known to concentrate free magnetic energy along underlying neutral lines and represent the fundamental magnetic structure of CME precursors (Mackay et al. 2010). At the solar limb, filament channels oriented along the line of sight extend up into the corona and manifest as dark cavities in emission. **B_{LOS} in coronal cavities is a measure of stored magnetic free energy** (see, e.g., Corchado-Albelo et al. 2021).

Coronal cavities have been associated with eruptions involving both bipolar and quadrupolar configurations (Fig. 4; Yurchyshyn 2002; Vršnak et al. 2004; Gibson et al. 2006; Maričić et al. 2009; Gibson 2015; 2017; Karna et al. 2021). They occur frequently throughout the solar cycle (Fig. 5) even with an observational bias toward cavities aligned with the observer's line of sight; this useful selection effect favors ~axisymmetric geometries, facilitating identification of X-points (Fig. 3) and O-points (Fig. 6). Ruminska et al. (2022) analyzed >1000 coronal cavities and found >80% of 570 unique cavities had CoMP lagomorphic signatures during their lifetime. **Coronal cavities are ideal candidates for the study of pre-eruption magnetic structures.**

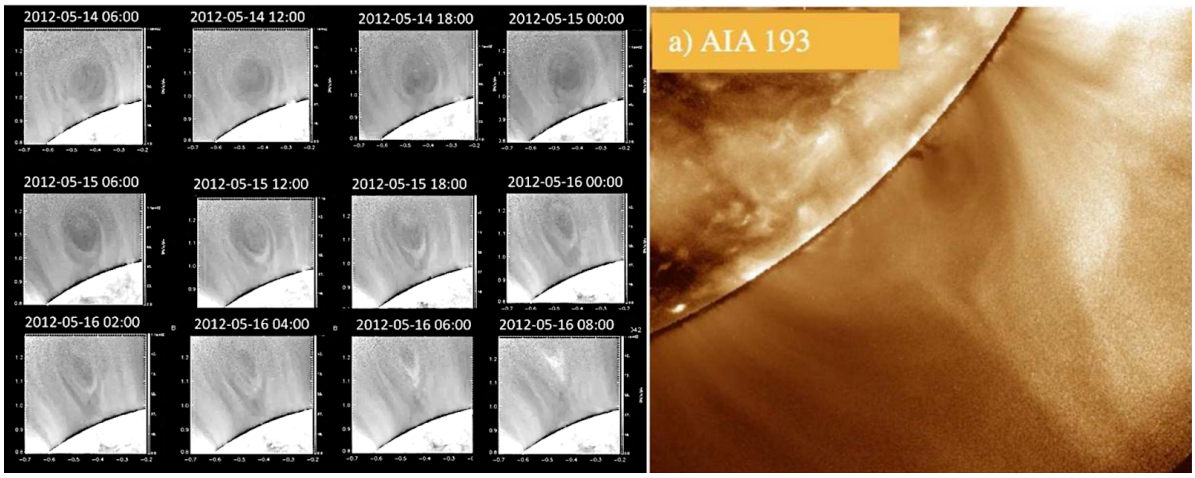

Fig. 4. Cavities ultimately erupt as CMEs. (Left) Long-lived cavity with slow activation phase; hours leading up to eruption (Gibson 2015; high-res). (Right) Quadrupolar pseudostreamer w/ coronal cavity (north lobe) that erupts following day (Karna et al. 2021; high-res).

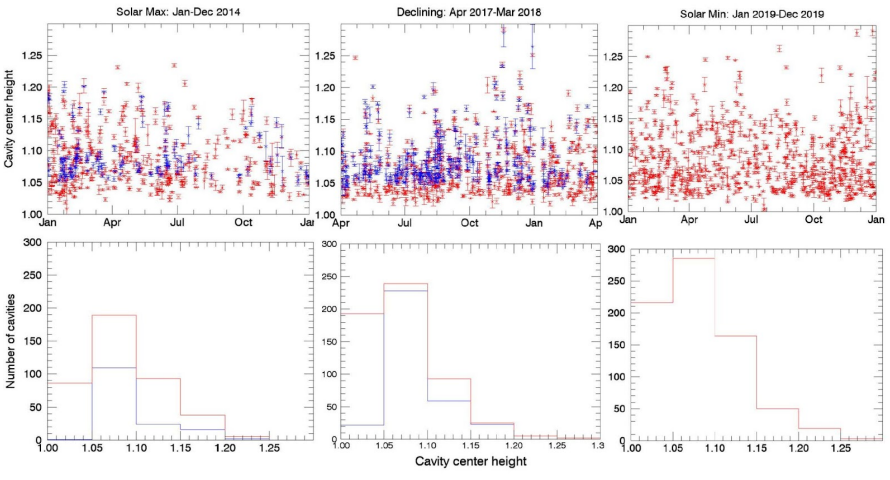

Fig. 5. Cavities are ubiquitous. (Top) A survey of coronal cavities vs time for three solar cycle periods using (red) SDO/AIA and (blue) CoMP Fe XIII intensity observations. (Bottom) Histograms for the three time periods. Note CoMP is an occulted coronagraph> 1.05 solar radii; also that CoMP was not observing in 2019. See Ruminska et al. (2022); high-res.

Finding: Coronal cavities are ubiquitous throughout the solar cycle, erupt as CMEs, and have coronal polarimetric signatures that distinguish between model predictions.
Recommendation: Coronal cavities should be targeted in a comprehensive multiwavelength study of CME precursors and associated eruption-driving mechanisms.

3. The Solution, Part Two: Finding Xs and Os in Coronal Cavities

In line-of-sight-aligned coronal cavities, the identification of magnetic O-points is a straightforward matter of looking for circular contours in B_{LOS}. Simulations where a pre-eruption cavity is identified with a magnetic flux rope (Fig. 6, top) demonstrate that a ~10-25 Gauss field aligned with the cavity axis (B_{LOS}) is sufficient to drive a torus-instability CME with acceleration and final speed within the observed range (Bein et al. 2011; Fan 2018; Fan & Liu 2019). In contrast, sheared-arcade simulations with a magnetic breakout topology (quadrupole with X point above it; Fig. 6, bottom) store magnetic energy well below the cavity center with very little B_{LOS} higher in the corona. Thus, although both models in Fig. 6 have one or more magnetic O-points, **the existence and location of the O- and X-points relative to the cavity center distinguish between flux rope and sheared arcade models, and thus CME drivers.**

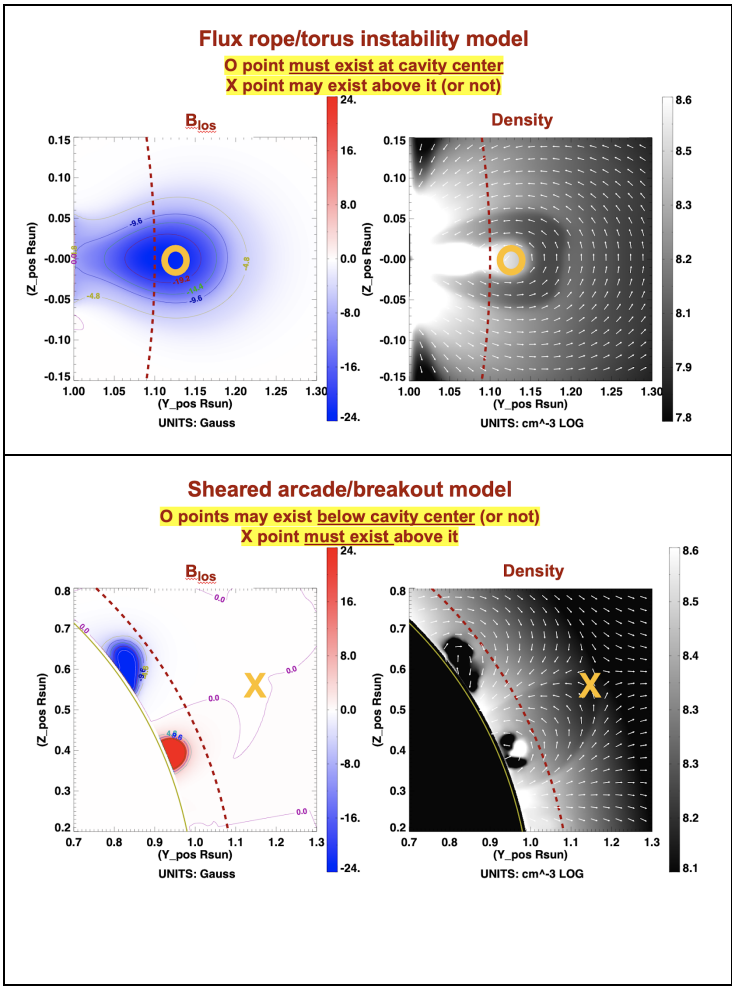

Fig. 6. B_{LOS} distinguishes between CME models.

(Top) Fan & Liu (2019) flux rope model of coronal cavity and underlying prominence (prominence lies below the red dashed line reference height of 1.1 R_{sun}). Note the O-point topology seen in circular contours of B_{LOS} (left; high-res) and field lines (right) coincides with the center of the elliptical cavity seen in density (right; high-res).

(Bottom) Dahlin et al. (2021) sheared arcade/quadrupolar breakout topology simulation. Here O-points form at the beginning of eruption (shortly after time step shown) and are associated with the lower-lying field concentrations of the filament channel and not the center of the density-depleted cavities. An X-point lies above the two magnetic lobes, as expected in a quadrupolar magnetic topology. High-res (left, right).

B_{LOS} in coronal cavities has never been observed. In VIR, a ground-based telescope with significantly bigger aperture than the 20-cm CoMP is needed to measure the faint circular polarization (V/I) signal and allow direct inversion of B_{LOS} (Fan et al., 2018). The **4m Daniel K. Inouye Solar Telescope (DKIST)** provides an exciting new opportunity to measure the magnetic structure of small cavities for the first time, but is unlikely to capture an eruption because of its small field of view. The proposed **1.5m Coronal Solar Magnetism Observatory Large Coronagraph (COSMO-LC)** has a ***global field of view dedicated to synoptic coronal observations*** and so is ideally suited to studies of CMEs and their precursors (see *white paper by Tomczyk et al., 2022*). Fig. 7 shows forward-modeled circular polarization with and without photon noise added for the COSMO telescope as in Fan et al. 2018 (note a weaker-field (10 G) flux rope was used in that study vs. Fan & Liu (2018; 24 G)). Even for these relatively low intensity/magnetic field strength structures, a 1-min integration time resolves the magnitude of the axial field (Fig. 7 b), and with a 5-min integration time (more than sufficient to capture evolution on time scales of cavity eruptions, see Fig. 4, left), the B_{LOS} maximum at 1.1 Rs (O-point) is resolved. **The proposed 1.5m COSMO-LC has the sensitivity, spatial and temporal resolution to measure magnetic field evolution on a ~1-min time scale, and to detect and follow the presence and height of a magnetic O-point during the slow rise phase of a magnetic flux rope erupting as a CME.**

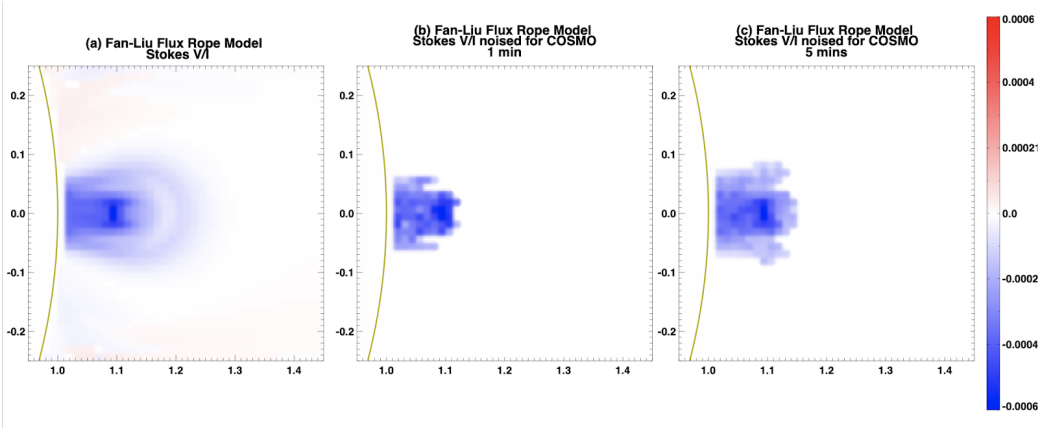

Fig. 7. Circular polarization can be inverted to obtain B_{LOS}. (a) Fan & Liu (2019) forward modeled circularly polarized light (V/I); compare to B_{LOS} of Fig 6 (top) (high-res). (b) Same with photon noise for the 1.5m COSMO telescope with 1-min integration time, 12" resolution, system efficiency=.05, and modulation efficiency=1/√3 (high-res). (d) Same for 5-min integration time (high-res). For a discussion of complementary radio polarimetric diagnostics, see *white paper by Chen et al. 2022*.

Finding: The **4m Daniel K. Inouye Solar Telescope (DKIST)** and proposed **1.5m Coronal Solar Magnetism Observatory Large Coronagraph (COSMO-LC)** make a major leap forward in VIR coronal sensitivity, enabling measurement of **B.**
Recommendation: A dedicated coronal synoptic telescope with a large field-of-view (i.e., **COSMO-LC**) is needed to identify the dominant CME driving mechanisms, by observing coronal magnetic fields from precursor state into eruption.

In the UV, space-borne instruments can take advantage of the fact that the H I Lyman-α (Lyα) coronal line is the strongest UV emission from the Sun, extending far out from the solar surface. The sensitivity of Lyα to the unsaturated Hanle effect yields a measurement of B_{LOS} that is independent of the Zeeman effect measured by VIR circular polarization. Instead, it is based on the rotation of the linear polarization direction (Azimuth) from the solar limb tangent (Raouafi et al. 2016; Zhao et al. 2019). The **12-cm Coronal Lyman-α Resonance Observatory (CLARO**; see *white paper by Casini et al. 2022)* utilizes an internally occulted Lyα coronagraph to be deployed to the International Space Station (ISS). Because of the brightness of the Lyα corona and its strong linear polarization by resonance scattering, despite its small aperture, CLARO is sufficiently sensitive to measure B_{LOS} in coronal cavities and distinguish between the flux rope and sheared arcade models (Fig. 8). As the first solar coronal mission dedicated to the observation of linearly polarized light by resonance scattering in the UV, CLARO would demonstrate the diagnostic power of Lyα coronal spectropolarimetry. With its relatively small size, such an instrument could be deployed to vantage points off the Sun-Earth line (see COMPLETE *white papers by Caspi et al. 2022*) and potentially even over the Sun's poles, where B_{LOS} would provide a unique view on the important geoeffective quantity B_Z. **CLARO's coronal Lyα spectropolarimetry provides a coronal magnetic diagnostic that complements those from large ground-based VIR telescopes, small enough to be deployed throughout the heliosphere, building a 4π view of the coronal magnetic field.**

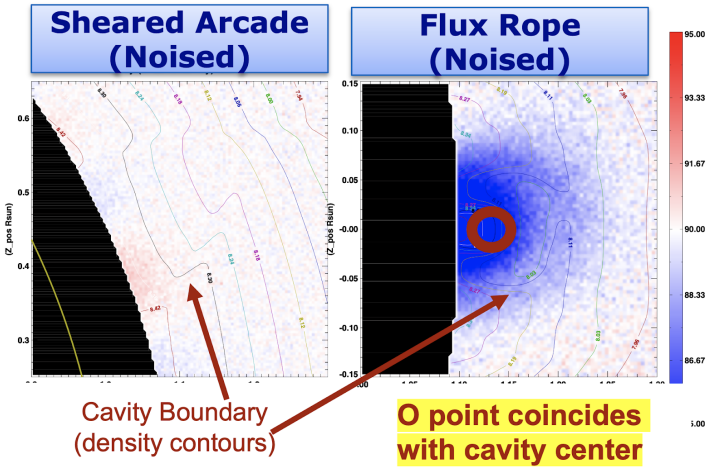

Fig. 8. Forward modeling demonstrates that CLARO can distinguish between models of CME precursors. Forward-modeled Lyα linear polarization Azimuth (vector direction; scales with B_{LOS}) for sheared-arcade (left; high-res) and flux-rope (right; high-res) simulations as shown in Fig. 6, with photon noise added and determined for a 12 cm telescope, 1.5 hour integration, 3.5" pixels, and 0.0074 flux throughput. Contours of simulation density in the plane of sky are overplotted to identify spatial location of cavity relative to Lyα Azimuth signal.

Finding: The proposed 12-cm **Coronal Lyman-α Resonance Observatory (CLARO)** spectropolarimetric coronagraph demonstrates a path forward for space-based observations of the coronal magnetic field, which may be incorporated into future missions away from the Sun-Earth line (e.g., **COMPLETE**).

Recommendation: In order to provide an independent and complementary coronal magnetic diagnostic to large ground-based telescopes measurements, small-telescope spectropolarimetric capability in the unsaturated Hanle regime should be explored.

References

Antiochos, S. K., DeVore, C.R., Klimchuk, J.A. (1999) *ApJ*, 510, 485
https://iopscience.iop.org/article/10.1086/306563

Bąk-Stęślicka U, Gibson, S. E., Fan, Y., Bethge, C., Forland, B., Rachmeler, L. A. (2013) *ApJ*, 770, 28 https://iopscience.iop.org/article/10.1088/2041-8205/770/2/L28

Bein, B. M. et al (2011) *ApJ,* 738, 191
https://iopscience.iop.org/article/10.1088/0004-637X/738/2/191

Bommier, V. and Sahal-Bréchot, S. (1982) *Sol. Phys.,* 78, 157
https://articles.adsabs.harvard.edu/full/1982SoPh...78..157B

Casini, R., et al. (2022) *A White Paper Submitted to the Solar and Space Physics Decadal Survey*

Casini, R. and Judge, P. G. (1999) *ApJ*, 522, 524
https://iopscience.iop.org/article/10.1086/307629

Caspi, A., et al. (2022a,b) *A White Paper Submitted to the Solar and Space Physics Decadal Survey*

Casini, R., White, S., and Judge, P. (2017) *SSR*, 210, 145
https://link.springer.com/article/10.1007/s11214-017-0400-6

Corchado-Albelo, M. F., Dalmasse, K., Gibson, S., Fan, Y., and Malanushenko, A. (2021) *ApJ,* 907, 23 https://iopscience.iop.org/article/10.3847/1538-4357/abc8f0

Chen, B. et al. (2020) *Nature Astron.*, DOI:10.1038/s41550-020-1147-7/2020
https://ui.adsabs.harvard.edu/abs/2020NatAs...4.1140C/abstract

Chen, B., et al., (2022) *A White Paper Submitted to the Solar and Space Physics Decadal Survey*

Dalmasse et al. (2019), *ApJ,* 877, 111
https://iopscience.iop.org/article/10.3847/1538-4357/ab1907

De Rosa, M. L. et al. (2009), *ApJ*, 696, 1780
https://iopscience.iop.org/article/10.1088/0004-637X/696/2/1780

Dahlin, J. T., DeVore, C. R. and Antiochos, S. K. (2021) 2021arXiv211200641
https://arxiv.org/abs/2112.00641

Dima, G. and Schad, T. (2020) *ApJ,* 889, 109
https://iopscience.iop.org/article/10.3847/1538-4357/ab616f

Fan, Y and Gibson, S. E. (2007) *ApJ*, 668, 1232
https://iopscience.iop.org/article/10.1086/521335

Fan, Y. (2018) MHD Simulation of Prominence Eruption, *ApJ*, 862, 54
https://iopscience.iop.org/article/10.3847/1538-4357/aaccee

Fan, Y., Gibson, S., Tomczyk, S. (2018) *ApJ*, 866, 57
https://iopscience.iop.org/article/10.3847/1538-435

Fan, Y., and Liu, T. (2019) *Front. Astron. Space Sci.*, 6, 27
https://www.frontiersin.org/articles/10.3389/fspas.2019.00027/full

Fineschi, S., Hoover, R. B., Fontenla, J. M., & Walker, A. B. C. 1991, *OptEn*, 30, 1161
https://ui.adsabs.harvard.edu/abs/1991SPIE.1343..376F/abstract

Fineschi, S., Hoover, R. B., Zukic, M., et al. 1993, *Proc. SPIE*, 1742, 423
https://ui.adsabs.harvard.edu/abs/1993SPIE.1742..423F/abstract

Gibson, S. (2015) *ASSL*, 415, 323
https://link.springer.com/chapter/10.1007/978-3-319-10416-4_13

Gibson S. E., Foster D, Burkepile J, de Toma G, Stanger A (2006) *ApJ*, 641, 590
https://iopscience.iop.org/article/10.1086/500446

Gibson, S., et al. (2017) *ApJL*, 840, 13
https://iopscience.iop.org/article/10.3847/2041-8213/aa6fac

Gibson, S., et al. (2021) White Paper Submitted to Helio2050
https://www.hou.usra.edu/meetings/helio2050/pdf/4062.pdf

Ishikawa, R. et al. (2021) *Sci. Adv.*, 7, 8
https://www.science.org/doi/10.1126/sciadv.abe8406

Kano, R. et al. (2017) *ApJL*, 839, L10
https://iopscience.iop.org/article/10.3847/2041-8213/aa697f

Karna, N., (2021) *ApJ*, 913, 47
https://iopscience.iop.org/article/10.3847/1538-4357/abf2b8

Karpen, J. T., Antiochos, S. K., and DeVore, C. R. (2012) *ApJ*, 760, 81
https://iopscience.iop.org/article/10.1088/0004-637X/760/1/81

Kliem, B., & Török, T. (2006) *Phys. Rev. Lett.*, 96, 255002
https://journals.aps.org/prl/abstract/10.1103/PhysRevLett.96.255002

Lin, H., Penn, M. J., and Tomczyk, S. (2000) *ApJL,* 541, L42
https://iopscience.iop.org/article/10.1086/312900

Lin, H., Kuhn, J. R., and Coulter, R., *ApJL*, 613, L177, 2004
https://iopscience.iop.org/article/10.1086/425217

Lynch, B. J., Edmondson, J. K., Kazachenko, M. D., Guidoni, S. E. (2016) *ApJ,* 826, 43
https://iopscience.iop.org/article/10.3847/0004-637X/826/1/43

Mackay, D. H., Karpen, J. T., Ballester, J. L., Schmieder, B., and Aulanier, G. (2010) *Space Sci. Rev.*, 151, 4, 333–399
https://ui.adsabs.harvard.edu/abs/2010SSRv..151..333M/abstract

Maričić D, Vršnak B, Roša D (2009) *Solar Phys.* 260, 177
https://link.springer.com/article/10.1007/s11207-009-9421-y

Paraschiv A.R. and Judge P. G. (2022) *Solar Phys*. 297, 63
https://link.springer.com/article/10.1007/s11207-022-01996-5

Patsourakos, S., Vourlidas, A., Török, T. et al. (2020) *Space Sci Rev,* 216, 131
https://link.springer.com/article/10.1007/s11214-020-00757-9

Plowman, J. (2014) *ApJ*, 792, 23
https://iopscience.iop.org/article/10.1088/0004-637X/792/1/23/meta

Rachmeler, L. A., Gibson, S. E., Dove, J. B., DeVore, C. R. and Fan, Y. (2013) *Solar Phys.* 288, 617
https://link.springer.com/article/10.1007/s11207-013-0325-5

Rachmeler, L. A., Casini, R., and Gibson, S. E. (2012) *ASPC*, 463, 227
https://opensky.ucar.edu/islandora/object/articles:18959

Raouafi, N.-E., Sahal-Bréchot, S., Lemaire, P., *A&A,* 396, 1019, 2002
https://ui.adsabs.harvard.edu/abs/2002A%26A...396.1019R/abstract

Raouafi, N. E., Riley, P., Gibson, S., Fineschi, S. and Solanki, S. K. (2016) *Front. Astron. Space Sci.,* 20
https://www.frontiersin.org/articles/10.3389/fspas.2016.00020/full

Ruminska, A., Bąk-Stęślicka U, Gibson, S. E. and Fan, Y. (2022), *ApJ,* 926, 146
https://iopscience.iop.org/article/10.3847/1538-4357/ac469c

Tomczyk, S., Card, G. L., Darnell T., Elmore, D. F., Lull, R., Nelson, P. G., Streander, K. V., Burkepile, J., Casini, R., Judge, P. G. (2008) *Solar Phys.,* 247, 411
https://link.springer.com/article/10.1007/s11207-007-9103-6

Tomczyk, S. et al. (2022) *A White Paper Submitted to the Solar and Space Physics Decadal Survey*

Trujillo Bueno, J., Landi Degl'Innocenti, E., and Belluzzi, L. (2017), *SSRv*, 210, 183
https://link.springer.com/article/10.1007/s11214-016-0306-8

Vršnak B, Maričić D, Stanger AL, Veronig A (2004) Solar Phys., 225, 355
https://link.springer.com/article/10.1007/s11207-004-4995-x

Woodgate, B. E. et al. (1980) Solar Phys,. 65, 73
https://ui.adsabs.harvard.edu/abs/1980SoPh...65...73W/abstract

Yang, Z. et al. (2020a) Science, 369, 694, 2020
https://www.science.org/doi/10.1126/science.abb4462

Yang, Z. et al. (2020b) Sci China Tech Sci, 63, 2357
https://link.springer.com/article/10.1007/s11431-020-1706-9

Yurchyshyn VB (2002) ApJ., 576, 4
https://iopscience.iop.org/article/10.1086/341628

Zhao, J., Gibson, S. E., Fineschi, S., Susino, R., Casini, R., Li, Hui, Gan, W. (2019) ApJ, 883, 55
https://iopscience.iop.org/article/10.3847/1538-4357/ab328b